Numerical solution of Lower bound theorem

Hao Wu*, Zhipei Zhang

Yellow River Engineering Consulting Co., Ltd., Zhengzhou, Henan 450003, China

*250320158@qq.com

Abstract. A numerical solution for solving plastic stress field based on the lower bound theorem is proposed in this paper. The method uses the node equilibrium equations rather than the element equilibrium equations. The equilibrium differential equations over the area of element around the node are transformed into the equilibrium integral equations along the boundary by Green's theorem. A linear programming model is developed with the variables of nodes stresses, linearized objective functions, equilibrium equations, stress boundary conditions and yield criteria constraints. The lower bound limit load and plastic stress field can be computed from the model. The further analysis shows that it is necessary only for the element equilibrium equations to introduce the node unique to a particular element, which will cause the model suitable only for the lower bound limit load, not for the plastic stress field. For the node equilibrium equations, it is not necessary to introduce the node unique to a particular element. The model with the node equilibrium equations is suitable for both the lower bound limit load and the plastic stress field. One example for the lower bound limit load and the plastic stress field illustrates the capability of the numerical solution proposed in this paper.

Keywords: Lower bound theorem; Numerical solution; Node equilibrium equations; Limit load; Plastic stress field; Degree of relative freedom

1 Introduction

Drucker and Prager[1] proposed the lower bound theorem of classical plasticity theory in 1951. The lower bound theorem assumes a perfectly rigid-plastic model and states that any statically admissible stress field will furnish a lower bound estimate of the true limit load. Lysmer[2] proposed a linear programming model for solving stability problems using the lower bound theorem based on the idea of the finite element method and the linearization of Mohr-Coulomb yield criterion in 1970. Wai-fah Chen[3] elaborated the application of limit analysis method in geotechnical problems in his monograph Limit Analysis and Soil Plasticity published in 1975. Sloan[4] solved the foundation bearing capacity problem based on the active set algorithm in 1988, and gived the solution of the stability problem.

As a particularly useful tool for the analysis of stability, lower bound theorem has attracted the interest from many researchers in view of its simplicity and more

H. Bilgin et al. (eds.), *Proceedings of the 2023 5th International Conference on Civil Engineering, Environment Resources and Energy Materials (CCESEM 2023)*, Advances in Engineering Research 227,
https://doi.org/10.2991/978-94-6463-316-0_23

importantly by-passing the cumbersome time-history elastoplastic analyses, whilst still providing the failure mechanisms of the structures involved[5, 6, 7, 8].

Based on the numerical solution presented by Lysmer and Sloan, lower bound theorem has been extensively used in a wide variety of problems, such as tunnels[9, 10, 11], slopes[12, 13, 14], foundations[15, 16, 17], anchors[18, 19] and braced excavations[20, 21]. Li's research proposed to use the 4-noded triangular elements instead of 3-noded triangular elements for meshing while the assumption of the node unique to particular element is remained[22].

The present research about the lower bound theorem is basically focused on solving the stability problems of geotechnical engineering based on the lower bound theorem, including the stability of slope or underground cavern, the bearing capacity of foundation and the earth pressure of retaining structure. Very few resaerch involves the plastic stress field. The plastic stress field under the action of limit load is necessary and important for the reinforcement measures in engineering, espicailly under the case that the stability of geotechnical engineering cannot meet the requirements.

This paper presents a numerical method named limit element method (LEM for short) for solving plastic stress field based on the lower bound theorem. LEM uses the node equilibrium equations rather than the element equilibrium equations. The equilibrium differential equations over the area of element around the node are transformed into the equilibrium integral equations along the boundary by Green's theorem. A linear programming model is developed with the variables of nodes stresses, linearized objective functions, equilibrium equations, stress boundary conditions and yield criteria constraints. The lower bound limit load and plastic stress field can be computed from the model. The further analysis shows that it is necessary only for the element equilibrium equations to introduce the node unique to a particular element, which will cause the model suitable only for the lower bound limit load, not for the plastic stress field. For the node equilibrium equations, it is not necessary to introduce the node unique to a particular element. The linear programming model with the node equilibrium equations is suitable for both the lower bound limit load and the plastic stress field. One example for the lower bound limit load and the plastic stress field illustrates the capability of LEM.

2 Lower bound theorem and mathematical model

2.1 Lower bound theorem

The lower bound theorem of classical plasticity theory assumes a perfectly plastic soil model and states that any statically admissible stress field will furnish a lower bound estimate of the true limit load. A statically admissible stress field is one which satisfies (a) the stress boundary conditions, (b) equilibrium, and (c) the yield condition.

2.2 Mathematical model

For the body of volume V with surface S, the mathematical model of the lower bound theorem can be written as follow

$$\begin{aligned} \max \quad & Q(\sigma) \\ \text{st.} \quad & E(\sigma) = b_V \\ & B(\sigma) = b_S \\ & F(\sigma) \le 0 \end{aligned} \tag{1}$$

where
σ - stress in V;
$Q(\sigma)$ - objective function;
$E(\sigma) = b_V$, equilibrium differential equation;
$B(\sigma) = b_S$, stress boundary conditions;
$F(\sigma) \le 0$, yield criterion.

The mathematical model of the lower bound theorem Eq. (1) (LBM for short) is an optimization model.

3 Plastic stress field

3.1 Optimization model

The feasible solution is one which satisfies all the constraints of the optimization model. The maximum value of the objective function of the optimization model is referred to as the maximum value. The optimal solution is one which maximizes the objective function. For an optimization model, the feasible solution may exist or not. If the feasible solution does not exist, the optimal solution does not exist; If the feasible solution exists, the maximum value may exist (finite) or not (infinite). If the maximum value exists, the optimal solutions exist, and the quantity of the optimal solutions may be finite or infinite.

3.2 Plastic stress field

The feasible solution of LBM corresponds to the statically admissible stress field of the lower bound theorem. The maximum value of LBM corresponds to the lower bound limit load of the lower bound theorem. The optimal solution of LBM corresponds to the lower bound limit stress field of the lower bound theorem. The lower bound limit stress field is one which satisfies all the constraints of LBM under the condition of the lower bound limit load.

Plastic point of the lower bound theorem is one which is in yield state in any lower bound limit stress field. Otherwise it is a non-plastic point. The area composed of all plastic points only is called plastic zone.

The physical meaning of the plastic point is one which has to be in yield state under the action of the lower bound limit load. The physical meaning of plastic zone is one which has to be in yield state under the action of lower bound limit load.

Due to the convexity of the yield criterion, the lower bound limit stress field in the plastic zone is unique, while the lower bound limit stress field in the non-plastic zone is not unique. The plastic stress field is the stress field in the plastic zone under the lower bound limit load.

3.3 Numerical solution for the LBM

Due to the complexity of practical problems, it is generally difficult to achieve the analytical solution of the LBM. The numerical method presented by Lysmer and Sloan (Sloan method for short) is often used in practical. Sloan method is only suitable for computing the lower bound limit load, non-suitable for the plastic stress field due to its model. A numerical solution of the LBM named as limit element method (LEM for short) is proposed in this paper, which is not only suitable for computing the lower bound limit load but also for the plastic stress field.

4 Brief review of Sloan method.

In Sloan method, the soil is discretized into a collection of 3-noded triangular elements with the nodal unique to particular element and the variables being the unknown stresses. Statically admissible stress discontinuities are permitted to occur at the interfaces between adjacent triangles. Application of the stress-boundary conditions, equilibrium equations and yield criterion lead to an expression for the collapse load which is maximized subject to a set of linear constraints on the stresses. In order to avoid nonlinear constraints occurring in the constraint matrix, the yield criterion must be expressed as a linear function of the unknown stresses. For Mohr-Coulomb yield criteria, this is achieved by employing a polygonal approximation to the yield surface. The polygon is defined so that it lies inside the parent yield surface, thus ensuring that the solution obeys the conditions of the lower bound theorem.

4.1 Meshes and the node unique to particular element

In Sloan method, the triangular elements are used to model the stress field under conditions of plane strain. A mesh of linear stress triangles is shown in Fig. 1. Unlike the usual form of the finite element method, each node is unique to a particular element and more than one node may share the same co-ordinates. Statically admissible stress discontinuities are permitted at shared edges between adjacent triangles. If E denotes the number of triangles in the mesh, then there are 3E nodes and 9E unknown stresses.

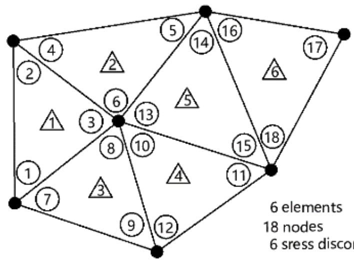

Fig. 1. Mesh of triangles of Sloan method

4.2 Variables

Variables are all the nodes stresses, denoted as σ_n.

4.3 Objective functions

Linear objective function is employed as follow in Sloan method:

$$C^T\sigma_n \tag{2}$$

where C^T is the objective vector.

4.4 Element equilibrium equations

The variation of the stress throughout each triangular element is linear and each node is associated with 3 unknown stresses of σ_x, σ_y and τ_{xy}. Each stress varies throughout an element according to

$$\sigma_x = \sum_{i=1}^{3} N_i\sigma_{xi}, \quad \sigma_y = \sum_{i=1}^{3} N_i\sigma_{yi}, \quad \tau_{xy} = \sum_{i=1}^{3} N_i\tau_{xyi} \tag{3}$$

where
σ_x, σ_y, τ_{xy} - the nodal stresses;
N_i - linear shape functions.

According to the static equilibrium differential equations, the element equilibrium equations can be written as follow:

$$A_1\sigma_n = b_1 \tag{4}$$

4.5 Stress boundary conditions

The stress boundary conditions can be written as follow:

$$A_2\sigma_n = b_2 \tag{5}$$

4.6 Yield condition

Assuming tensile stresses are taken as positive and plane strain conditions, the Mohr-Coulomb yield criterion may be expressed as

$$(\sigma_x - \sigma_y)^2 + (2\tau_{xy})^2 - (2c \cdot \cos\varphi - (\sigma_x + \sigma_y)\sin\varphi)^2 \le 0 \tag{6}$$

The linearized Mohr-Coulomb yield criterion can be written as follow

$$A_k\sigma_x + B_k\sigma_y + C_k\tau_{xy} \le D \tag{7}$$

where

$$A_k = \cos(2\pi k/p) + \sin\varnothing\cos(\pi/p)$$
$$B_k = \sin\varnothing\cos(\pi/p) - \cos(2\pi k/p)$$
$$C_k = 2\sin(2\pi k/p)$$
$$D = 2c\cos\varnothing\cos(\pi/p)$$
$$k = 1,2,\ldots,p$$

The linearized Mohr-Coulomb yield criterion can be written as follow:

$$A_3\sigma_n \le b_3 \tag{8}$$

4.7 Discontinuity equilibrium

In order to permit statically admissible discontinuities at the edges of adjacent triangles, it is necessary to enforce additional constraints on the nodal stresses. A statically admissible discontinuity permits the tangential stress to be discontinuous, but requires that continuity of the corresponding shear and normal components is preserved. Fig. 2 illustrates two triangles, a and b, which share a side d defined by the nodal pairs (1, 2) and (3, 4). Since the stresses vary linearly along each element edge, this condition is equivalent to enforcing the constraints

$$\sigma_{n1}^a = \sigma_{n2}^b,\quad \sigma_{n3}^a = \sigma_{n4}^b,\quad \tau_1^a = \tau_2^b,\quad \tau_3^a = \tau_4^b \tag{9}$$

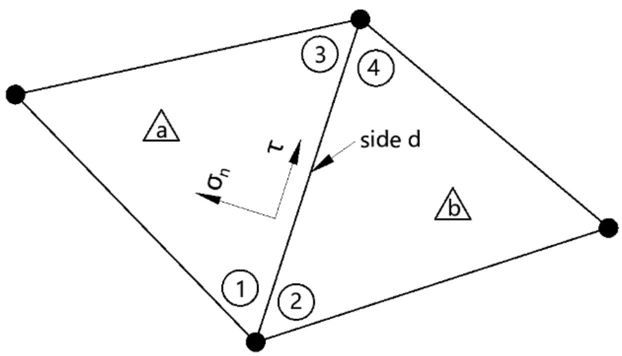

Fig. 2. Discontinuity equilibrium between adjacent triangles

The linearized discontinuity equilibrium can be written as follow:

$$A_4\sigma_n = b_4 \tag{10}$$

4.8 Linear programming model

With the linearized equilibrium equation constraints, the linearized stress boundary conditions, linearized yield criterion, discontinuity equilibrium and linearized objective function, the linear programming model of the lower bound theorem can be written as follow

$$\begin{aligned} \max \quad & C^T\sigma_n \\ \text{st.} \quad & A_1\sigma_n = b_1 \\ & A_2\sigma_n = b_2 \\ & A_3\sigma_n \le b_3 \\ & A_4\sigma_n = b_4 \end{aligned} \tag{11}$$

where
σ_n - global vector of nodal stresses;
C^T - objective vector;
$A_1\sigma_n = b_1$, equilibrium equation constraints;
$A_2\sigma_n = b_2$, stress boundary condition constraints;
$A_3\sigma_n \le b_3$, yield criterion constraints;
$A_4\sigma_n = b_4$, discontinuity equilibrium constraints.

4.9 Solution of lower bound limit load and plastic stress field

The mathematical model of Sloan's method is a linear programming model, and the maximum value of the objective function is the lower bound limit load.

Due to the node unique to particular element in Sloan method, each feasible solution of the linear programming model has multiple groups of node stresses at the same node coordinates, resulting in that the feasible solution of the linear programming model cannot form a statically admissible stress field. Therefore, Sloan method is only suitable for solving the limit load, not for solving the plastic stress field.

5 Limit element method

5.1 Mesh

Triangular elements are used to model the stress field under conditions of plane strain, which is like the usual form of the finite element method but different from Sloan method. Each node with stresses σ_x, σ_y and τ_{xy} is co-owned by the elements around the node rather than unique to a particular element. A mesh of triangular elements is shown in Fig. 3. If E denotes the quantity of the nodes in the mesh, then there are 3E unknown stresses.

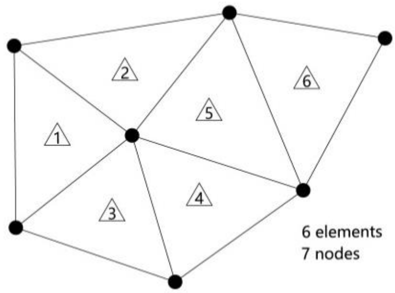

Fig. 3. Mesh of triangular of LEM

5.2 Node equilibrium equations

Static equilibrium differential equations are as follow

$$\frac{\partial \sigma_x}{\partial x} + \frac{\partial \tau_{xy}}{\partial y} = b_X \tag{12}$$
$$\frac{\partial \tau_{xy}}{\partial x} + \frac{\partial \sigma_y}{\partial y} = b_Y$$

By integrating Eq. (12) over the area D of the element around the node, the following equations can be achieved

$$\iint_D \left(\frac{\partial \sigma_x}{\partial x} + \frac{\partial \tau_{xy}}{\partial y}\right) dxdy = \iint_D b_X dxdy \tag{13}$$
$$\iint_D \left(\frac{\partial \tau_{xy}}{\partial x} + \frac{\partial \sigma_y}{\partial y}\right) dxdy = \iint_D b_Y dxdy$$

Green theorem is as follow

$$\iint_D \left(\frac{\partial Q}{\partial x} - \frac{\partial P}{\partial y}\right) dxdy = \oint_L Pdx + Qdy \tag{14}$$

According to the Eq. (13) and Eq. (14), the following can be achieved

$$\oint_L (-\tau_{xy})dx + \sigma_x dy = \iint_D b_X dxdy \tag{15}$$

$$\oint_L (-\sigma_y)dx + \tau_{xy} dy = \iint_D b_Y dxdy \tag{16}$$

where
L –boundary of area D of the element around the node.

Eq. (15) and Eq. (16) are the static node equilibrium integral equations. In Eq. (15), $\oint_L (-\tau_{xy})dx$ denotes the resultant force of the shear stress τ_{xy} around the boundary of the area D in X direction; and $\oint_L \sigma_x dy$ denotes the resultant force of the normal stress σ_x around the boundary of the area D in X direction; and $\iint_D b_X dxdy$ denotes the resultant body force in area D in X direction. In Eq. (9), $\oint_L (\tau_{xy})dx$ denotes the resultant force of the shear stress τ_{xy} around the boundary of the area D in Y direction; and $\oint_L (-\sigma_y)dy$ denotes the resultant force of the normal stress σ_y around the boundary of the area D in Y direction; and $\iint_D b_Y dxdy$ denotes the resultant body force in area D in Y direction.

The Eq. (15) and Eq. (16) shows that the resultant force of the stresses around the boundary of the area D equals to the resultant body force over the area D in X direction and Y direction respectively.

The stresses vary linearly along the element boundary. The normal stress σ_x and the shear stress τ_{yx} along the triangular boundary are shown in Fig. 4. The normal stress σ_y and the shear stress τ_{xy} along the triangular boundary are shown in Fig. 5.

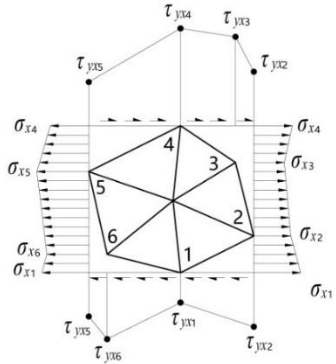

Fig. 4. Normal stress σ_x and shear stress τ_{yx} along the triangular boundary

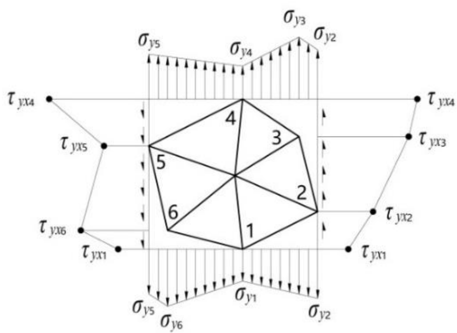

Fig. 5. Normal stress σ_y and shear stress τ_{xy} along the triangular boundary

According to Eq. (15) and Eq. (16), node equilibrium equations can be achieved as follow:

$$[A^e][\sigma^e] = [b^e] \tag{17}$$

where

$$[A^e] = \begin{bmatrix} \eta_1 & 0 & \zeta_1 & \eta_2 & 0 & \zeta_2 & \eta_3 & 0 & \zeta_3 & \eta_4 & 0 & \zeta_4 & \eta_5 & 0 & \zeta_5 & \eta_6 & 0 & \zeta_6 \\ 0 & \zeta_1 & \eta_1 & 0 & \zeta_2 & \eta_2 & 0 & \zeta_3 & \eta_3 & 0 & \zeta_4 & \eta_4 & 0 & \zeta_5 & \eta_5 & 0 & \zeta_6 & \eta_6 \end{bmatrix};$$

$$[\sigma^e] = [\sigma_{x1} \quad \sigma_{y1} \quad \tau_{xy1} \quad \sigma_{x2} \quad \sigma_{y2} \quad \tau_{xy2} \quad \sigma_{x3} \quad \sigma_{y3} \quad \tau_{xy3} \quad \sigma_{x4} \quad \sigma_{y4} \quad \tau_{xy4} \quad \sigma_{x5} \quad \sigma_{y5} \quad \tau_{xy5} \quad \sigma_{x6} \quad \sigma_{y6} \quad \tau_{xy6}]$$

$$[b^e] = \left[\iint_D b_X dxdy \quad \iint_D b_Y dxdy\right]^T;$$

$$\eta_1 = \frac{1}{2}(y_2 - y_6); \quad \eta_2 = \frac{1}{2}(y_3 - y_1);$$
$$\eta_3 = \frac{1}{2}(y_4 - y_2); \quad \eta_4 = \frac{1}{2}(y_5 - y_3);$$
$$\eta_5 = \frac{1}{2}(y_6 - y_4); \quad \eta_6 = \frac{1}{2}(y_1 - y_5);$$
$$\zeta_1 = \frac{1}{2}(x_6 - x_2); \quad \zeta_2 = \frac{1}{2}(x_1 - x_3);$$
$$\zeta_3 = \frac{1}{2}(x_2 - x_4); \quad \zeta_4 = \frac{1}{2}(x_3 - x_5);$$
$$\zeta_5 = \frac{1}{2}(x_4 - x_6); \quad \zeta_6 = \frac{1}{2}(x_5 - x_1).$$

Assembling all the node equilibrium integral equations for the overall meshes into constraint matrix, the overall equilibrium constraints matrix can be achieved as follow

$$A_1\sigma_n = b_1 \tag{18}$$

5.3 Stress boundary conditions

The stress boundary conditions can be written as follow:

$$A_2\sigma_n = b_2 \tag{19}$$

5.4 Yield condition

The Mohr-Coulomb yield criterion can be linearized as follow

$$A_3\sigma_n \le b_3 \tag{20}$$

5.5 Objective function

The objective function may be written as follow

$$C^T\sigma_n \tag{21}$$

5.6 Linear programming model

According to Eq. (18), Eq. (19), Eq. (20) and Eq. (21), the linear programming model of the lower bound theorem can be written as follow

$$\begin{aligned} \max \quad & C^T\sigma_n \\ \text{st.} \quad & A_1\sigma_n = b_1 \\ & A_2\sigma_n = b_2 \\ & A_3\sigma_n \le b_3 \end{aligned} \tag{22}$$

where
σ_n - variables, the stresses σ_x, σ_y and τ_{xy} of the nodes;
C^T - objective vector;
$A_1\sigma_n = b_1$, equilibrium equations constraints;
$A_2\sigma_n = b_2$, stress boundary conditions constraints;
$A_3\sigma_n \le b_3$, yield criterion constraints.

6 Discussion on Sloan method and LEM

6.1 Preparations - degree of relative freedom

According to the linear theory, for a linear equations with n variables and m equations

$$A_{m\times n}x_{n\times 1} = b_{m\times 1} \tag{23}$$

there are conclusions as follow:
(1) if rank $[A_{m\times n}]$ = rank $[A_{m\times n} \quad b_{m\times 1}] < n$, the Eq. (23) has infinite solutions;
(2) if rank $[A_{m\times n}]$ = rank $[A_{m\times n} \quad b_{m\times 1}] = n$, the Eq. (23) has unique solution;
(3) if rank $[A_{m\times n}]$ < rank $[A_{m\times n} \quad b_{m\times 1}]$, the Eq. (23) has no solution.
The linear equilibrium equations produced by the Sloan method or LEM are as follow

$$A_{m\times n}\sigma_{n\times 1} = b_{m\times 1} \tag{24}$$

The degree of relative freedom is defined as

$$F_r = \frac{n}{m} \tag{25}$$

where
F_r– degree of relative freedom;
n – quantity of variables in Eq. (25);
m – quantity of equations in Eq. (25).
Based on the Eq. (23), the following statements are acceptable
(1) if $F_r > 1$, the Eq. (25) has infinite solutions;
(2) if $F_r = 1$, the Eq. (25) has unique solution;
(3) if $F_r < 1$, the Eq. (25) has no solution.

6.2 Degree of Relative freedom of triangular elements

Triangular elements are employed for meshing without the assumption of the node unique to particular element.

Since the average internal angle degree of the triangular element is 60 °, as shown in Fig.6, there should be 360°/60°=6 elements around one node in average.

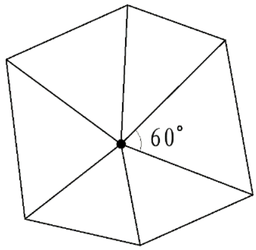

Fig. 6 Triangular elements around one node

For each node, there are 3 variables, σ_x, σ_y and τ_{xy}. The quantity of variables corresponding to each element may be regarded as 3/6=0.5. A triangular element has 3 nodes, so the average quantity of variables corresponding to one triangular element is 0.5×3=1.5. For each triangular element, the element equilibrium equations produce 2 equality constraints. According to Eq. (25), the degree of relative freedom is as follow

$$F_r = \frac{1.5}{2} = 0.75 \tag{26}$$

The element equilibrium equations has no solution since $F_r < 1$, so the lower bound limit load or the plastic stress field cannot be computed by the triangular element equations without the assumption of the node unique to particular element.

One example as shown in Fig. 7, a rectangular area is meshed with triangular elements without node unique to particular element. In the horizontal direction, it is discretized into m elements with m+1 nodes, and in the vertical direction, it is discretized into n elements with n+1 nodes. The total quantity of the variables is 3(m+1) (n+1), since each node has 3 variables σ_x, σ_y and τ_{xy}. The total quantity of equality constraints of the equilibrium equation is 4mn, since there are 2mn elements and each element has 2 equilibrium equations.

The linear equilibrium equations produced by the lower bound theorem are as follow

$$A_{(4mn)\times(3(m+1)\,(n+1))}\sigma_{(3(m+1)\,(n+1))\times 1} = b_{(4mn)\times 1} \tag{27}$$

The degree of relative freedom of Eq. (27) is as follow

$$F_r = \frac{3(m+1)(n+1)}{4mn} \tag{28}$$

If m and n are both large enough, $F_r \approx \frac{3}{4} < 1$. The Eq. (27) has no solution since $F_r < 1$, so the lower bound limit load or the plastic stress field cannot be computed by the triangular element equations without assumption of the node unique to particular element.

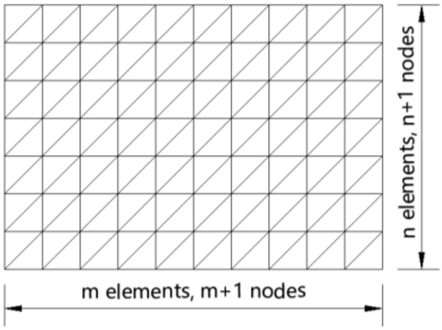

Fig. 7 Triangular elements in rectangular

6.3 Degree of relative freedom of Sloan method

Triangular elements are employed for meshing with the assumption of the node unique to particular element, which is inevitably associated with the discontinuity equilibrium.

For each node, there are 3 variables, σ_x, σ_y and τ_{xy}. A triangular element has 3 nodes, so the total quantity of variables corresponding to one triangular element is 3 × 3=9.

The equilibrium equations produce 2 equality constraints on each element.

The discontinuity equilibrium produces 4 equality constraints on each common edge of adjacent triangular elements, so there are 2 equality constraints corresponding to one element. Each triangular element has 3 common edges on average, so the discontinuous equilibrium produces 6 equality constraints on one triangular element on average. Therefore, a triangular element has total 8 equality constraints on average. According to Eq. (25), the degree of relative freedom is as follow

$$F_r = \frac{9}{8} = 1.125 \quad (29)$$

The element equilibrium equations has infinite solutions since $F_r > 1$, so the lower bound limit load or the plastic stress field can possibly be computed by Sloan method.

One example as shown in Fig. 7, a rectangular area is meshed with the assumption of the node unique to particular element. In the horizontal direction, it is discretized into m elements with m+1 nodes, and in the vertical direction, it is discretized into n elements with n+1 nodes. There are 2mn elements and each element has 9 variables σ_x, σ_y and τ_{xy}, so the total quantity of the variables is 18mn.

There are 2mn elements and each element has 2 equilibrium equations, so the quantity of equilibrium equation constraints is 4mn. The mesh has 3mn-m-n common edges of adjacent triangular elements, so the discontinuous equilibrium produces 12mn-4m-4n equality constraints. The total quantity of equality constraints is 16mn-4m-4n.

The linear equilibrium equations constraints generated by the lower bound theorem are as follow

$$A_{(16mn-4m-4n)\times(18mn)}\sigma_{(18mn)\times 1} = b_{(16mn-4m-4n)\times 1} \tag{30}$$

The degree of relative freedom of Eq. (30) is as follow

$$F_r = \frac{18mn}{16mn-4m-4n} \tag{31}$$

The Eq. (30) has infinite solutions since $F_r \approx \frac{18}{16} > 1$, so the lower bound limit load and the plastic stress field can possibly be computed by Sloan method.

6.4 Degree of relative freedom of LEM

For each node, there are 3 variables, σ_x, σ_y and τ_{xy}, and the node equilibrium equations produce 2 equality constraints. According to Eq. (25), the degree of relative freedom is as follow

$$F_r = \frac{3}{2} = 1.5 \tag{32}$$

The Eq. (32) has infinite solutions since $F_r > 1$, so the lower bound limit load or the plastic stress field can possibly be computed by LEM method.

One example as shown in Fig. 7, a rectangular area is meshed with triangular elements without node unique to particular element. In the horizontal direction, it is discretized into m elements with m+1 nodes, and in the vertical direction, it is discretized into n elements with n+1 nodes. The total quantity of the variables is 3(m+1) (n+1), since each node has 3 variables σ_x, σ_y and τ_{xy}. The total quantity of equality constraints of the equilibrium equation is 2(m+1) (n+1), since there are (m+1) (n+1) nodes and each node has 2 equilibrium equations.

The linear equilibrium equations constraints generated by the lower bound theorem are as follow

$$A_{2(m+1)(n+1)\times 3(m+1)(n+1)}\sigma_{3(m+1)(n+1)\times 1} = b_{2(m+1)(n+1)\times 1} \tag{33}$$

The degree of relative freedom of Eq. (33) is as follow

$$F_r = \frac{3(m+1)(n+1)}{2(m+1)(n+1)} \tag{34}$$

The Eq. (33) has infinite solutions since $F_r = \frac{3}{2} > 1$, so the lower bound limit load and the plastic stress field can possibly be computed by LEM.

6.5 Discussion

The key difference between LEM and Sloan method is the equilibrium equations type, which will lead to the following results:

(1) If element equilibrium equations are employed for triangular element meshing without the assumption of the node unique to particular element, the model has no solution, so the lower bound limit loads or the plastic stress field cannot be computed.

(2) If element equilibrium equations are employed for triangular element meshing with the assumption of the node unique to particular element, which is inevitably associated with the discontinuity equilibrium, the LBM has infinite solutions, so the lower bound limit loads and the plastic stress field can possibly be computed.

(3) If node equilibrium equations are employed for triangular meshing without the assumption of the node unique to particular element, the model has infinite solutions, so the lower bound limit loads and the plastic stress field can possibly be computed.

(4) The assumption of the node unique to particular element is only inevitable by the element equilibrium equations rather than the node equilibrium equations.

(5) Each feasible solution of LEM produces a statically admissible stress field. A series of statically admissible stress field can be achieved.

(6) The feasible solution of the Sloan method does not produce the statically admissible stress field due to the node unique to particular element.

7 Examples

7.1 Bearing capacity of strip foundation

The bearing capacity of a strip foundation can be described as an evenly distributed load of a certain width applied on the surface of a horizontal foundation with an infinite length.

The following data are used: horizontal direction: a width of 50 m, discretized into 50 elements with a width of 1 m; vertical direction: a height of 10 m, discretized into 10 elements with a width of 1 m; the evenly distributed load is located in the middle of the top, and the width of the load is 20 m, as shown in Fig. 8.

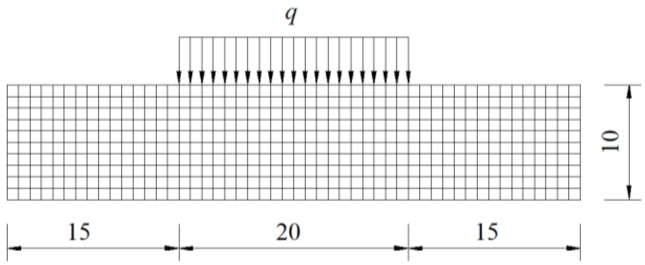

Fig. 8 Model for bearing capacity of cohesive foundation

When the soil $\gamma = 0$ and internal friction degree $\varphi = 0$, the lower bound limit load can be achieved by the Prandtl's solution Eq. (33):

$$\frac{q}{c} = \pi + 2 \tag{35}$$

Based on LEM, the lower bound limit load $\frac{q}{c} = 4.7836$, while the Prandtl's solution $\frac{q}{c} = 5.1416$. The relative error is 6.96%. The example shows that LEM has good capacity.

7.2 Plastic stress field

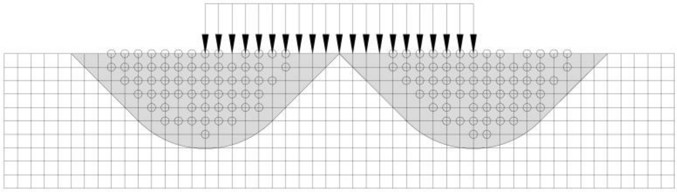

Fig. 9 Plastic stress field

The plastic zone of the strip foundation given by slip line under the action of ultimate load is shown in the shaded area in Figure 9. The plastic nodes computed by LEM are shown with circle point in Figure 9, and the other nodes are non-plastic nodes. It can be seen that LEM has applicability for solving plastic stress field.

8 Conclusion

LEM for solving plastic stress field based on the lower bound theorem is proposed in this paper. LEM uses the node equilibrium equations rather than the element equilibrium equations. The equilibrium differential equations over the area of element around the node are transformed into the equilibrium integral equations along the boundary by Green's theorem. A linear programming model is developed with the variables of nodes stresses, linearized objective functions, equilibrium equations, stress boundary conditions and yield criteria constraints. The lower bound limit load and plastic stress field can be computed from the model. The further analysis shows that it is necessary only for the element equilibrium equations to introduce the node unique to a particular element, which will cause the linear programming model suitable only for the lower bound limit load, not for the plastic stress field. For the node equilibrium equations, it is not necessary to introduce the node unique to a particular element. The linear programming model with the node equilibrium equations is suitable for both the lower bound limit load and the plastic stress field. One example for the lower bound limit load and the plastic stress field illustrates the capability of LEM.

References

1. Drucker DC, Greenberg HJ, Prager W. The safety factor of an elastic-plastic body in plane strain. Journal of Applied Mechanics Transactions of the ASME, 1951, 18(4): 371-378.

2. J. Lysmer Limit analysis of plane problems in soil mechanics. J Soil Mech Found Div 96:1311–1334(1970). https://doi.org/10.1061/JSFEAQ.0001441.
3. Wai-fah Chen. Limit analysis and soil plasticity. Elsevier scientific publishing company, 1975.
4. S.W. Sloan. Lower bound limit analysis using finite elements and linear programming. International journal for numerical and analytical methods,vol.12:61–77 (1988). https://doi.org/10.1002/nag.1610120105.
5. Aguinaldo Fraddosio, Nicola Lepore, Mario Daniele Piccioni, Thrust Surface Method: An innovative approach for the three-dimensional lower bound Limit Analysis of masonry vaults, Engineering Structures, Volume 202, 2020, 109846, ISSN 0141-0296, https://doi.org/10.1016/j.engstruct.2019.109846.
6. Jianfeng Zhou, Junxing Wang, Lower bound limit analysis of wedge stability using block element method, Computers and Geotechnics, Volume 86, 2017, Pages 120-128, ISSN 0266-352X, https://doi.org/10.1016/j.compgeo.2016.12.031.
7. Boonchai Ukritchon, Suraparb Keawsawasvong, Three-dimensional lower bound finite element limit analysis of Hoek-Brown material using semidefinite programming, Computers and Geotechnics, Volume 104, 2018, Pages 248-270, ISSN 0266-352X, https://doi.org/10.1016/j.compgeo.2018.09.002.
8. K.D. Nikolaou, K. Georgiadis, C.D. Bisbos, Lower bound limit analysis of 2D steel frames with foundation–structure interaction, Engineering Structures, Volume 118, 2016, Pages 41-54, ISSN 0141-0296, https://doi.org/10.1016/j.engstruct.2016.03.037.
9. Rui Sun, Junsheng Yang, Shouhua Liu, Feng Yang, Undrained stability analysis of dual unlined horseshoe-shaped tunnels in non-homogeneous clays using lower bound limit analysis method, Computers and Geotechnics, Volume 133, 2021, 104057, ISSN 0266-352X, https://doi.org/10.1016/j.compgeo.2021.104057.
10. Boonchai Ukritchon, Suraparb Keawsawasvong, Stability of unlined square tunnels in Hoek-Brown rock masses based on lower bound analysis, Computers and Geotechnics, Volume 105, 2019, Pages 249-264, ISSN 0266-352X, https://doi.org/10.1016/j.compgeo.2018.10.006.
11. Boonchai Ukritchon, Suraparb Keawsawasvong, Lower bound solutions for undrained face stability of plane strain tunnel headings in anisotropic and non-homogeneous clays, Computers and Geotechnics, Volume 112, 2019, Pages 204-217, ISSN 0266-352X, https://doi.org/10.1016/j.compgeo.2019.04.018.
12. Nuno Deusdado, Armando N. Antão, Mário Vicente da Silva, Nuno Guerra, Application of the Upper and Lower-bound Theorems to Three-dimensional Stability of Slopes, Procedia Engineering, Volume 143, 2016, Pages 674-681, ISSN 1877-7058, https://doi.org/10.1016/j.proeng.2016.06.097.
13. Katsuhiko Arai, Mitsuo Nakagawa, A New Limit Equilibrium Analysis of Slope Stability Based on Lower-Bound Theorem, Soils and Foundations, Volume 28, Issue 1, 1988, Pages 1-15, ISSN 0038-0806, https://doi.org/10.3208/sandf1972.28.1.
14. Mohammad Reza Arvin, Faradjollah Askari, Orang Farzaneh, Seismic behavior of slopes by lower bound dynamic shakedown theory, Computers and Geotechnics, Volume 39, 2012, Pages 107-115, ISSN 0266-352X, https://doi.org/10.1016/j.compgeo.2011.08.001.

15. Ahmad Foroutan Kalourazi, Ardavan Izadi, Reza Jamshidi Chenari, Seismic bearing capacity of shallow strip foundations in the vicinity of slopes using the lower bound finite element method, Soils and Foundations, Volume 59, Issue 6, 2019, Pages 1891-1905, ISSN 0038-0806, https://doi.org/10.1016/j.sandf.2019.08.014.
16. K.D. Nikolaou, K. Georgiadis, C.D. Bisbos, Lower bound limit analysis of 2D steel frames with foundation–structure interaction, Engineering Structures, Volume 118, 2016, Pages 41-54, ISSN 0141-0296, https://doi.org/10.1016/j.engstruct.2016.03.037.
17. Suraparb Keawsawasvong, Sothoan Yoang, Boonchai Ukritchon, Rungkhun Banyong, Lower bound analysis of rectangular footings with interface adhesion factors on nonhomogeneous clays, Computers and Geotechnics, Volume 147, 2022, 104787, ISSN 0266-352X, https://doi.org/10.1016/j.compgeo.2022.104787.
18. V.N. Khatri, J. Kumar, Effect of anchor width on pullout capacity of strip anchors in sand, Can. Geotech. J. 48 (3) (2011) 511–517.
19. R.S. Merifield, S.W. Sloan, The ultimate pullout capacity of anchors in frictional soils, Can. Geotech. J. 43 (8) (2006) 852–868.
20. F.G. Degwitz, Numerical Upper and Lower Bound Limit Analysis for Braced Excavations, Massachusetts Institute of Technology, 2004.
21. B. Ukritchon, A.J. Whittle, S.W. Sloan, Undrained stability of braced excavations in clay, J. Geotech.
22. Chunguang Li, Cong Sun, Cuihua Li, Hong Zheng, Lower bound limit analysis by triangular elements, Journal of Computational and Applied Mathematics, Volume 315, 2017, Pages 319-326, ISSN 0377-0427, https://doi.org/10.1016/j.cam.2016.11.024.